Physics Letters A 383 (2019) 2938–2942

Contents lists available at ScienceDirect

Physics Letters A

www.elsevier.com/locate/pla

Energy band modulation of GaAs/$Al_{0.26}Ga_{0.74}As$ quantum well in 3D self-assembled nanomembranes

Fei Zhang [a], GaoShan Huang [a,*], XiaoFei Nie [b], Xin Cao [c], Zhe Ma [d], Fei Ding [c], ZengFeng Di [d], HongLou Zhen [b], YongFeng Mei [a,*]

[a] Department of Materials Science, State Key Laboratory of ASIC and Systems, Fudan University, Shanghai 200433, People's Republic of China
[b] State Key Laboratory of Infrared Physics, Shanghai Institute of Technical Physics, Chinese Academy of Sciences, Shanghai 200083, People's Republic of China
[c] Institut für Festkörperphysik, Leibniz Universität Hannover, Appelstrasse 2, 30167, Hannover, Germany
[d] State Key Laboratory of Functional Materials for Informatics, Shanghai Institute of Microsystem and Information Technology, Chinese Academy of Sciences, Shanghai 200050, People's Republic of China

ARTICLE INFO

Article history:
Received 12 March 2019
Received in revised form 5 June 2019
Accepted 24 June 2019
Available online 28 June 2019
Communicated by M. Wu

Keywords:
Quantum well
Nanomembrane
Energy band
Strain
Stark effect

ABSTRACT

In this study, we investigate the modulation of energy band in 3D self-assembled nanomembranes containing GaAs/$Al_{0.26}Ga_{0.74}As$ quantum wells (QWs). Photoluminescence (PL) characterizations demonstrate that the self-assembled structures have different optical transition properties and the modulation of the energy band is thus realized. Detailed spectral analyses disclose that the small strain change in structures with different curvatures cannot cause remarkable change in energy bands in $Al_{0.26}Ga_{0.74}As$ layer. On the other hand, the optical transitions of GaAs QW layer is influenced by the strain evolution in term of light emission intensity. We also find the first order Stark effect in rolled-up nanomembrane with diameter of 150 μm, which is closely connected with the coupling effect between the deformation potential and the piezoelectric potential. Our work may pave a way for the fabrication of high performance rolled-QW infrared photo-detectors.

1. Introduction

Quantum well (QW) is a type of low-dimensional semiconductor material which is artificially modified by energy band engineering. The low-dimensional properties, such as quantum size effect, quantum tunneling, Coulomb blocking, and nonlinear optical effect, are the basis of new generation of solid-state quantum devices, like QW infrared photo-detectors (QWIPs), lasers based on QW materials, etc. [1–10]. However, in conventional QW devices, only the incident light whose electric vector is parallel to the growth direction of the QW contributes to the photo-current, and so the quantum efficiency of the opto-electric device is low. In our previous work, we combined rolled-up nanotechnology with QW devices to fabricate microtubular QWIPs [11]. We notice that the view angle of the rolled-up device is remarkably expanded without much attenuation and quantum efficiency is also enhanced due to the internal light reflection or optical resonance in the microtubular cavities [12–17]. It is worth mentioning that the modulation of the energy band structure can significantly change the physical properties of QW for various applications. In previous literatures, several approaches have been demonstrated to modulate the energy band. For instance, strain in self-rolled nanomembranes is capable of altering the properties of the materials [17–20]. In addition, the change in the composition may also influence the band structure and the doping level and the electrical properties were tuned significantly [21,22]. Nevertheless, specific study about the modulation of the energy band of QWs and its effect on intraband and interband carrier transitions are still short so far. It is of great theoretical and application significance to investigate them in more details, so that clues may be found for optimizing the performance of the QWIP or preparing new type of QW devices. The 3D self-assembled nanomembrane structures are expected to provide a good platform for studying the relationship between the energy band modulation of QWs and the intraband & interband carrier transitions because the geometry and the strain status in the QW nanomembrans can be tuned controllably.

In this study, we fabricate 3D self-assembled nanomembrane structures with different geometries to study the energy band modulation mechanism of GaAs/$Al_{0.26}Ga_{0.74}As$ QW nanomembranes. We find the optical transition properties of the nanomembranes and the energy bands in $Al_{0.26}Ga_{0.74}As$ layer is not sensitive to the small curvatures change. However, the energy bands of GaAs QW layer move downward due to the strain evolution after release

* Corresponding authors.
E-mail addresses: gshuang@fudan.edu.cn (G. Huang), yfm@fudan.edu.cn (Y. Mei).

https://doi.org/10.1016/j.physleta.2019.06.034
0375-9601/

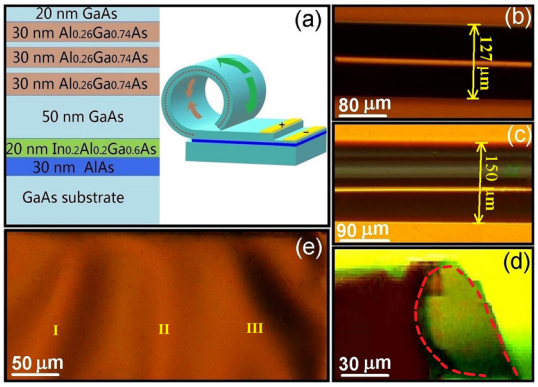

Fig. 1. (a) Schematic diagram of multi-layered nanomembrane and the self-rolled tubular structure with electrodes. The bottom part is GaAs substrate, and the dotted line is the neutral line which is the boundary between the parts with tensile and compressive strains respectively. Optical microscopy images (top view) of rolled-up structures with the diameter of (b) 127 μm and (c) 150 μm. The bright line on the black sample is reflected light. (d) A typical optical microscopy image of a rolled-down structure viewed from the side. The dotted line is the corresponding profile. (e) A typical optical microscopy image of a wrinkled nanomembrane (top view). The raised parts are marked with "I", "II", and "III".

of the pre-strained nanomembrane. The potential energy of electrons in rolled-up nanomembrane is also affected by the coupling effect between the deformation potential and the piezoelectric potential for self-rolled structures with different curvatures.

2. Experimental

The samples used are self-rolled nanomembrane structures with different geometries, in which the strain status can vary in a controllable way. The nanomembranes were fabricated using molecular beam epitaxy (Fig. 1(a)). Prior to the growth of the active nanomembrane, 200 nm GaAs buffer layer was grown at ~560 °C. For the epitaxial growth of the active nanomembrane, 30 nm AlAs sacrificial layer and 20 nm $In_{0.2}Al_{0.2}Ga_{0.6}As$ stress layer were firstly deposited. Then ~50 nm GaAs conductance layer followed as the bottom electrode (AuGe/Ni/Au). Finally, two QWs and 20 nm GaAs conductance layer (upper electrode) were deposited. Here, each QW is 6.5 nm GaAs layer wrapped by two 30 nm $Al_{0.26}Ga_{0.74}As$ layers (Fig. 1(a)). More details like the growth rates and temperatures and doping levels are presented in Supplementary Material A and B. Then, HF solution was used to etch away the AlAs sacrificial layer, and the nanomembrane is self-rolled by the strain release of $In_{0.2}Al_{0.2}Ga_{0.6}As$ stress layer due to the energy miniaturization of the system [23,24]. The device was then annealed at 380–400 °C to achieve a good electrical contact between metallic electrode and GaAs layer. Detailed fabrication process can be found in reference [11] and the Supplementary Material therein. Fig. 1(a) illustrates the schematic diagram of multi-layered nanomembrane and self-rolled tubular structure with electrodes fabricated by conventional semiconductor planar technology. Constant voltages of −3 and −4.5 V were also applied to such device to study the effect of external voltage on the optical transitions in the nanomembrane.

The morphologies of the 3D self-assembled nanomembranes were characterized by optical microscope (Olympus BX51). The photoluminescence (PL) properties of the samples were investigated using LabRAM HR spectrometer. The voltage was applied by battery pack during PL test.

3. Results and discussion

In our experiment, the self-assembly process initiated after the sacrificial AlAs layer was selectively removed by HF solution. We noticed that HF solutions with the concentrations of 13% and 15% led to the formation of rolled-up tubular structures with diameters of 127 μm (Fig. 1(b)) and 150 μm (Fig. 1(c)) respectively, while HF concentration below 10% caused the formation of rolled-down structure (Fig. 1d). In addition, it is experimentally proved that extended etching time could develop wrinkled structure (Fig. 1e). Table 1 summarizes the obtained geometries with different HF concentrations and etching times. Obviously, the different geometries of self-assembled structures result from different strain relaxation processes. Previous investigations also demonstrate that the strain gradient changes with the distance from the etching front [23,25] and the releasing history significantly influence the self-assembly process [26]. Thus, the current approach provides an alternative way to tune the geometry of self-assembled nanomembrane. For self-rolled nanomembrane with thickness t, the strain difference $\Delta\varepsilon$ can be expressed as $\Delta\varepsilon = t/((1+\nu)R_0)$, where ν represents Poisson ratio, R_0 is the radius of the structure. Herein, the average strain difference in the nanomembrane can be roughly estimated to be 0.12% and 0.10% for self-rolled nanoembranes with diameters of 127 and 150 μm respectively [27,28].

Table 1
Influence of HF concentrations and etching times on the geometries of the samples.

Sample	HF concentration	etching time (min)
127 μm rolled-up tube	13%	~4
150 μm rolled-up tube	15%	~3.5
wrinkled	>13%	>4
rolled-down tube	<10%	~7

Here, the energy band structures of the 3D self-assembled nanomembranes were studied by analyzing the PL spectra of the sample. First, the PL spectra of flat and rolled-up nanomembranes (diameter: 150 μm) are excited with high power laser (wavelength: 514.5 nm) at room temperature to study the high-energy transition of the carriers in the nanomembranes. Typical PL spectra is shown in Fig. 2(a). The spectra F and R_2 were collected with 7.5 mW excitation power while the excitation power for spectrum R_1 is 15 mW. According to the reference [29], the energy band gap of GaAs is around 1.42 eV, and the energy band gap of $Al_{0.26}Ga_{0.74}As$ layer should be larger. The high luminous flux (i.e., high laser power) can identify weaker peaks of $Al_{0.26}Ga_{0.74}As$ layer due to larger energy gap. On the basis of the spectral analyses, band diagrams of the $Al_{0.26}Ga_{0.74}As$ layer are schematically demonstrated in Fig. 2(b). Two sets of optical transitions can be deduced and the energy splitting is caused by the coupling between spin and angular momentum [30]. The left diagram in Fig. 2(b) is deduced according to the values of the transition energies (1.85–1.89 eV, 1.98–2.04 eV, and 2.15–2.20 eV) and it illustrates splitting of the energy levels which are produced by the coupling between resultant spin (L) and total orbital angular momentum quantum number (S) (i.e., LS coupling) among the outer electrons of atoms in the $Al_{0.26}Ga_{0.74}As$ layers [30,31]. The experimental results show that the smallest transition energy is 1.85 eV which is basically consistent with the values of $Al_xGa_{(1-x)}As$ reported previously [32].

The splitted energy levels in right panel of Fig. 2(b) are discrete and the transition energies are 2.374, 2.377, 2.390, and 2.400 eV which are deduced according to the peaks in the inset of Fig. 2(a). The difference between the first two transition energies is 0.003 eV (2.377–2.374 eV, see inet of Fig. 2(a)), which is consistent with the band splitting due to the coupling between the orbital angular momentum (l) and spin angular momentum (s) for the outer electrons only in one atom (i.e., ls coupling) [30]. On the other hand, the difference between adjacent transition energies for following 3 peaks is ~0.01 eV (see inset of Fig. 2(a)), which can be judged as degenerate energy level splitting brought by the Coulomb interactions between the electrons [30]. The splitted energy levels here indicates that the LS coupling is not particularly strong, otherwise,

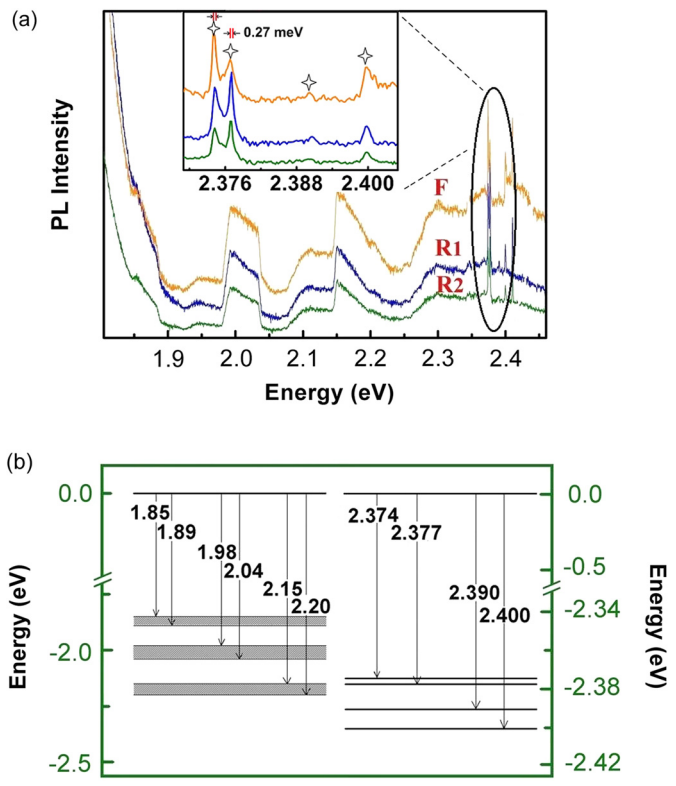

Fig. 2. (a) PL spectra at room temperature of flat (F) and rolled-up samples (diameter: 150 μm). Spectrum R_1 was collected with excitation power of 15 mW and spectra R_2 and F were collected with excitation power of 7.5 mW. The inset is the magnification of the elliptical part and the peaks are marked with the asterisks. Compared with the flat nanomembrane, the two peaks around 2.376 eV for rolled-up samples blue shift ~0.27 meV due to *ls* coupling of outer electrons. (b) Energy band diagram of $Al_{0.26}Ga_{0.74}As$ layer deduced from the PL results. (For interpretation of the colors in the figure(s), the reader is referred to the web version of this article.)

the broadening of the energy level might make the *ls* coupling undetectable. It is worth noting that in our present case the splitted energy levels should be produced by a coupling effect between *LS* coupling and *JJ* coupling if the electron configuration is taken into consideration [30]. After the formation of the rolled-up tubular structure by removing sacrificial layer, only the double lines take ~0.27 meV blueshift as a whole (Supplementary Material C) due to *ls* coupling and there is no change for the other transitions (inset of Fig. 2(a)). This phenomenon indicates that the *ls* coupling of outer electrons is sensitive to the strain change, while Coulomb interaction between the electrons in different atoms is almost unaffected. Therefore, the present experimental results prove that band structure is not very sensitive to the strain evolution, and the small strain change in self-assembled nanomembranes with small curvature difference is not large enough to change the energy levels of the $Al_{0.26}Ga_{0.74}As$ layer obviously. One may further deduce that similar situation may exist in both $Al_{0.26}Ga_{0.74}As$ and GaAs layers.

In order to observe the low-energy transition in the GaAs QW layer, the PL measurements were also carried out with 540 nm laser while the laser power was significantly decreased to 30 μW, and the obtained spectra were plotted in Fig. 3. Here spectra a-e correspond to the PL signal collected from different positions of a 3D self-assembled nanomembrane. It can be seen from Fig. 3(a) that with the decrease of the distance to the cut-off edge (position e), despite the intensity of PL spectrum increases gradually (possible due to different light scattering/reflection), the line shape keeps almost unchanged. Two obvious peaks can be distinguished and are considered to be due to the recombination between the electrons (*e*) and the heavy holes (*hh*) [25,33,34]. The ground and the first excited states of electrons are marked as e_0 and e_1 respectively while hh_0 and hh_1 for heavy hole case. The two peaks are therefore correspond to the e_0-hh_1 and e_1-hh_0 transitions respectively [25]. It is worth noting that the curvature gradually decreases from positions a to e, indicating a slightly changed strain status in the nanomembrane. However, the transition energies of e_0-hh_1 and e_1-hh_0 are almost the same in spectra a–e, although the corresponding strain status are different. This phenomenon further proves our previous deduction that the trivial strain change in the self-assembled nanomembrane cannot lead to obvious change of the energy levels. However, difference of transition energies in nanomemrbane before and after release can still be observed. Fig. 3(a) demonstrate that redshift can be observed in both $e_0 - hh_1$ and $e_1 - hh_0$ peaks after releasing the nanomembrane. This indicates that the ground state level e_0 and the excited state level e_1 move downward after release. A similar phenomenon is also observed in a wrinkled nanomembrane. For a clearer comparison, $e_1 - hh_0$ peaks of different measuring spots in a wrinkled nanomembrane are analyzed in detail, as shown in Fig. 3(b). According to our previous study [23], we consider that for the rolled-down part (position B, red spectrum), the two QWs are both under tensile strain while for the rolled-up part (position C, green spectrum), the two QWs are under compressive and tensile strains respectively. It can be seen from Fig. 3(b) that the $e_1 - hh_0$ peak in spectrum C appears blue shift compared with spectrum B. However, the flat part with two compressive QWs (spectrum A) demonstrates the highest $e_1 - hh_0$ transition energy, indicating the compressive strain can increase the transition energy. Another interesting feature in the PL behavior of the self-assembled nanomembranes is the obvious weakening of $e_0 - hh_1$ peak intensity after release (see spectra a-e in Fig. 3(a)). This phenonmenon illustrates that the strain not only changes the energy of level e_0 but also may decrease the possibility of associated electron transition.

For a QWIP device, a constant bias voltage may be applied. Therefore, it is also important to study the modulation of energy band when the self-assembled nanomembrane is biased. In present work, bias voltages of 0, −3, and −4.5 V were applied to the rolled-up nanomembranes, and the PL spectra excited with 540 nm laser were collected from the top of the rolled-up nanomembrane (Fig. 4). It can be seen from Fig. 4(a) that the $e_0 - hh_1$ peak is obviously stronger than $e_1 - hh_0$ peak for rolled-up nanomembrane with diameter of 127 μm when biased at −4.5 V. This is because high voltage and corresponding electric field can enforce the ground state wave function and the excited state wave function to the opposite directions, leading to the change of the relative intensity between $e_0 - hh_1$ and $e_1 - hh_0$ transitions [23,35]. However, for the rolled-up nanomembrane with diameter of 150 μm, strong $e_0 - hh_1$ peak is noted when 0 V is applied (see Fig. 4(b)). Obviously, the enhanced intensity cannot be connected with the strain status since the change in the diameter is small. From the point of PL line shape, it is observed that the 150 μm-tube with 0 V demonstrates a similar effect for 127 μm-tube with −4.5 V. We suggest this phenomenon may be produced by interfacial polarization, because the spectral profile can be affected by polarized perturbation [35]. In order to prove this speculation, we calculated the energy shift of the peaks when the samples were biased. Here, we focus on the ratio of the shift (with respect to 0 V) at −4.5 V to that at −3 V. For rolled-up nanomembrane with diameter of 127 μm, the ratio of the shift is ~2.14, which is close to the square of the voltage ratio (4.5 V/3 V). While in the case of rolled-up nanomembrane with diameter of 150 μm, the ratio of the shift is ~1.5. According to previous literature, a ratio close to 1.5 indicates the first order Stark effect, and a ratio close to 2.25 suggests the second order Stark effect [23]. We consider this

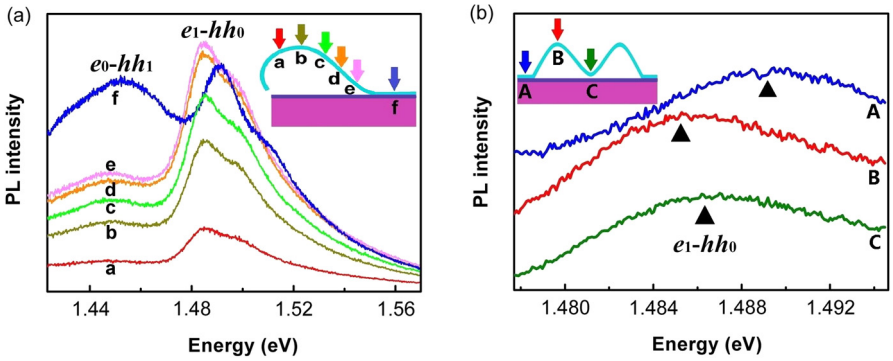

Fig. 3. (a) PL spectra of a rolled-down nanomembrane. (b) Enlarged view of e_1-hh_0 transitions of PL spectra for a wrinkled membrane. The colors of the plots correspond to the laser position marked by arrows with the same color (inset). Blue color corresponds to the result from the flat nanomembrane.

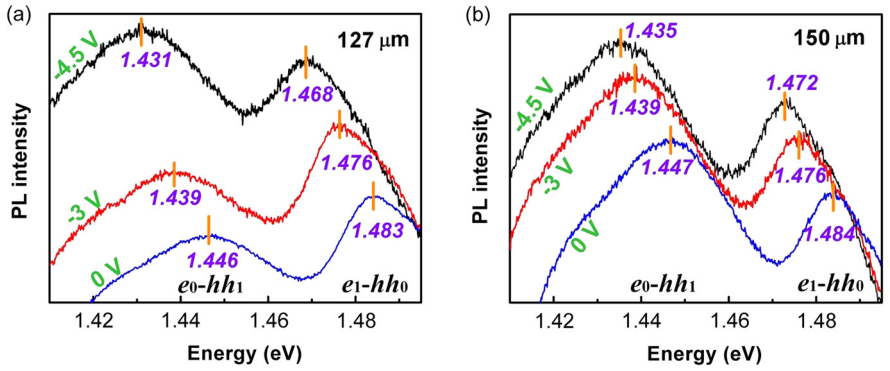

Fig. 4. PL spectra of rolled-up nanomembranes with diameters of 127 μm (a) and 150 μm (b) at room temperature. The excitation wavelength is 540 nm. Bias voltages of 0, −3, and −4.5 V were applied to the samples and the energies of e_0-hh_1 and e_1-hh_0 peaks are labeled.

may also exist in our experiment. The difference should originate from the 3D self-assembled geometry and the strain distribution therein. Specifically, the self-assembly process should produce deformation potential energy and the strain evolution in the GaAs and $Al_xGa_{(1-x)}As$ layers can induce a piezoelectric potential [36]. The coupling of the deformation potential and the piezoelectric potential will result in spatial anisotropy of electronic Hamiltonian to affect the depth of the potential minima of electrons [37–39]. The 3D self-assembled structures with different curvatures possess different strain distributions [28] and deformation potential, and the piezoelectric potential is also different correspondingly. As a result, the two structures demonstrate different piezoelectric behaviors.

4. Conclusions

The modulation of energy band for rolled QWs is studied in this work. On the basis of detailed PL characterization and analyses, two sets of energy levels for $Al_{0.26}Ga_{0.74}As$ layer can be deduced. We find that the small strain change for 3D self-assembled structures with different curvature alone cannot lead to obvious change in optical transition energy. The analyses of PL spectra of GaAs QW layer in different structures disclose that the ground state level e_0 and the excited state level e_1 will move downward due to the strain evolution after release of the pre-strained nanomembrane. Moreover, we suggest that the first order Stark effect might exist in rolled-up nanomembrane with diameter of 150 μm due to interfacial polarization. The results obtained in this work will facilitate to modulate the energy band of QW in 3D self-assembled nanomembranes for high performance QWIPs.

Acknowledgements

This work was financially supported by the National Natural Science Foundation of China (Nos. 61728501, 61805042, U1632115, and 51711540298), the China Postdoctoral Science Foundation (No. 2018M632014), the Science and Technology Commission of Shanghai Municipality (Nos. 18ZR1405100 and 17JC1401700), the Program of Shanghai Academic/Technology Research Leader (Nos. 16XD1404200 and 19XD1400600), the National Key Technologies R&D Program of China (No. 2015ZX02102-003), and the Changjiang Young Scholars Program of China. Part of the experimental work has been carried out in Fudan Nanofabrication Laboratory.

Appendix A. Supplementary material

Supplementary material related to this article can be found online at https://doi.org/10.1016/j.physleta.2019.06.034.

References

[1] Z. Cevher, P.A. Folkes, H.S. Hier, B.L. VanMil, B.C. Connelly, W.A. Beck, Y.H. Ren, Optimization of the defects and the nonradiative lifetime of GaAs/AlGaAs double heterostructures, J. Appl. Phys. 123 (2018) 161512.
[2] X.L. Zeng, J.L. Yu, S.Y. Cheng, Y.F. Lai, Y.H. Chen, W. Huang, Temperature dependence of photogalvanic effect in GaAs/AlGaAs two-dimensional electron gas at interband and intersubband excitation, J. Appl. Phys. 121 (2017) 193901.
[3] J. Faist, F. Capasso, D. Sivco, C. Sirtori, Quantum cascade laser, Science 264 (1994) 553–556.
[4] A. Hugi, G. Villares, S. Blaser, H.C. Liu, J. Faist, Mid-infrared frequency comb based on a quantum cascade laser, Nature 492 (2012) 229–233.
[5] L. Lin, H.L. Zhen, X.H. Zhou, N. Li, W. Lu, F.Q. Liu, An intermediate-band-assisted avalanche multiplication in InAs/InGaAs quantum dots-in-well infrared photodetector, Appl. Phys. Lett. 98 (2011) 073504.
[6] Q. Li, Z.F. Li, N. Li, X.S. Chen, P.P. Chen, X.C. Shen, W. Lu, High-polarization-discriminating infrared detection using a single quantum well sandwiched in plasmonic micro-cavity, Sci. Rep. 4 (2014) 6332.
[7] M. Geiser, J.L. Klocke, M. Mangold, P. Allmendinger, A. Hugi, P. Jouy, B. Horvath, J. Faist, T. Kottke, Single-shot microsecond-resolved spectroscopy of the bacteriorhodopsin photocycle with quantum cascade laser frequency combs, Biophys. J. 114 (2018) 173a.
[8] G. Villares, A. Hugi, S. Blaser, J. Faist, Dual-comb spectroscopy based on quantum-cascade-laser frequency combs, Nat. Commun. 5 (2014) 5192.

[9] L. Xia, V. Tokranov, S.R. Oktyabrsk, J.A. del Alamo, Experimental study of <110> uniaxial stress effects on p-channel GaAs quantum-well FETs, IEEE Trans. Electron Devices 58 (2011) 2597–2603.
[10] A.K. Fung, J.D. Albrecht, M.I. Nathan, P.P. Ruden, H. Shtrikman, In-plane uniaxial stress effects of AlGaAs/GaAs modulation doped heterostructures characterized by the transmission line method, J. Appl. Phys. 84 (1998) 3741–3746.
[11] H. Wang, H.L. Zhen, S.L. Li, Y.L. Jing, G.S. Huang, Y.F. Mei, W. Lu, Self-rolling and light-trapping in flexible quantum well-embedded nanomembranes for wide-angle infrared photodetectors, Sci. Adv. 2 (2016) e1600027.
[12] J. Zhang, J.X. Li, S.W. Tang, Y.F. Fang, J. Wang, G.S. Huang, R. Liu, L.R. Zheng, X.G. Cui, Y.F. Mei, Whispering-gallery nanocavity plasmon-enhanced Raman spectroscopy, Sci. Rep. 5 (2015) 15012.
[13] K. Dietrich, C. Strelow, C. Schliehe, C. Heyn, A. Stemmann, S. Schwaiger, S. Mendach, A. Mews, H. Weller, D. Heitmann, T. Kipp, Optical modes excited by evanescent-wave-coupled PbS nanocrystals in semiconductor microtube bottle resonators, Nano Lett. 10 (2010) 627–631.
[14] H.P. Ning, Y. Zhang, H. Zhu, A. Ingham, G.S. Huang, Y.F. Mei, A. Solovev, Geometry design, principles and assembly of micromotors, Micromachines (Basel) 9 (2018) 75.
[15] C. Ortix, J.V.D. Brink, Effect of curvature on the electronic structure and bound-state formation in rolled-up nanotubes, Phys. Rev. B 81 (2010) 165419.
[16] C. Strelow, C.M. Schultz, H. Rehberg, H. Welsch, C. Heyn, D. Heitmann, T. Kipp, Three dimensionally confined optical modes in quantum-well microtube ring resonators, Phys. Rev. B 76 (2007) 045303.
[17] C. Strelow, C.M. Schultz, H. Rehberg, M. Sauer, H. Welsch, A. Stemmann, C. Heyn, D. Heitmann, T. Kippl, Light confinement and mode splitting in rolled-up semiconductor microtube bottle resonators, Phys. Rev. B 85 (2012) 155329.
[18] J.H. Wong, B.R. Wu, M.F. Lin, Strain effect on the electronic properties of single layer and bilayer graphene, J. Phys. Chem. C 116 (2012) 8271–8277.
[19] Y.F. Mei, S. Kiravittaya, M. Benyoucef, D.J. Thurmer, T. Zander, C. Deneke, F. Cavallo, A. Rastelli, O.G. Schmidt, Optical properties of a wrinkled nanomembrane with embedded quantum well, Nano Lett. 7 (6) (2007) 1676.
[20] V.Y. Prinz, V.A. Seleznev, A.K. Gutakovsky, V.V. Preobrazhenskii, M.A. Putyato, T.A. Gavrilova, Free-standing and overgrown InGaAs/GaAs nanotubes, nanohelices and their arrays, Physica E 6 (2000) 828–831.
[21] S.B. Li, M. Ware, J. Wu, P. Minor, Z.M. Wang, Z.M. Wu, Y.D. Jiang, G.J. Salamo, Polarization induced pn-junction without dopant in graded AlGaN coherently strained on GaN, Appl. Phys. Lett. 101 (2012) 122103.
[22] S.B. Li, T. Zhang, J. Wu, Y.J. Yang, Z.M. Wang, Z.M. Wu, Z. Chen, Y.D. Jiang, Polarization induced hole doping in graded $Al_xGa_{1-x}N$ ($x = 0.7 \sim 1$) layer grown by molecular beam epitaxy, Appl. Phys. Lett. 102 (2013) 062108.
[23] F. Zhang, X.F. Nie, G.S. Huang, H.L. Zhen, F. Ding, Z.F. Di, Y.F. Mei, Strain-modulated photoelectric properties of self-rolled $GaAs/Al_{0.26}Ga_{0.74}As$ quantum well nanomembrane, Appl. Phys. Express 12 (2019) 065003.
[24] A. Malachias, C. Deneke, B. Krause, C. Mocuta, S. Kiravittaya, T.H. Metzger, O.G. Schmidt, Direct strain and elastic energy evaluation in rolled-up semiconductor tubes by x-ray microdiffraction, Phys. Rev. B 79 (2009) 03531.
[25] H.L. Zhen, G.S. Huang, S. Kiravittaya, S.L. Li, C. Deneke, D.J. Thurmer, Y.F. Mei, O.G. Schmidt, Light-emitting properties of a strain-tuned microtube containing coupled quantum wells, Appl. Phys. Lett. 102 (2013) 041109.
[26] I.S. Chun, A. Challa, B. Derickson, K. Jimmy Hsia, X.L. Li, Geometry effect on the strain-induced self-rolling of semiconductor membranes, Nano Lett. 10 (2010) 3927–3932.
[27] A. Pateras, J. Park, Y. Ahn, J.A. Tilka, M.V. Holt, C. Reichl, W. Wegscheider, T.A. Baart, J.P. Dehollain, U. Mukhopadhyay, L.M.K. Vandersypen, P.G. Evans, Mesoscopic elastic distortions in GaAs quantum dot heterostructures, Nano Lett. 18 (2018) 2780–2786.
[28] C. Peter, K. Suwit, M. Ingolf, S. Joachim, G.S. Oliver, Directional roll-up of nanomembranes mediated by wrinkling, Nano Lett. 11 (2011) 236–240.
[29] G.K. Vijaya, A. Alemu, A. Freundlich, Dilute nitride multi-quantum well multi-junction design: a route to ultra-efficient photovoltaic devices, in: Proceedings of SPIE-The International Society for Optical Engineering, 2011.
[30] H. Haken, H.C. Wolf, The Physics of Atoms and Quanta, Springer-Verlag, Herdelberg, 2005.
[31] J. Chen, W.Y. Zeng, Coupling effect of quantum wells on band structure, J. Semicond. 36 (2015) 102005.
[32] M.R. Aziziyan, W.M. Hassen, D. Morris, E.H. Frost, J.J. Dubowski, Photonic biosensor based on photocorrosion of GaAs/AlGaAs quantum heterostructures for detection of Legionella pneumophila, Biointerphases 11 (2016) 019301.
[33] X.Q. Li, T.H. Zhang, S. Mukamel, R.P. Mirin, S.T. Cundiff, Investigation of electronic coupling in semiconductor double quantum wells using coherent optical two-dimensional Fourier transform spectroscopy, Solid State Commun. 149 (2009) 361–366.
[34] C. Deneke, A. Malachias, S. Kiravittaya, M. Benyoucef, T.H. Metzger, O.G. Schmidt, Strain states in a quantum well embedded into a rolled-up microtube: X-ray and photoluminescence studies, Appl. Phys. Lett. 96 (2010) 143101.
[35] H.Q. Le, J.J. Zayhowski, W.D. Goodhue, Stark effect in $Al_xGa_{1-x}As/GaAs$ coupled quantum wells, Appl. Phys. Lett. 50 (1987) 1518–1520.
[36] B. Odekirk, Dielectric film stress influences on GaAs MESFET gate breakdown, in: Technical Digest-GaAs IC Symposium, 1992, pp. 195–198.
[37] J.H. Davies, I.A. Larkin, Theory of potential modulation in lateral surface superlattices, Phys. Rev. B 49 (1994) 4800.
[38] H.Y. Yao, G.H. Yun, W.L. Fan, Equilibrium piezoelectric potential of a bent ZnO nanowire based upon the stress consistency assumption, Mech. Compos. Mater. 51 (2015) 661–668.
[39] J.H. Davies, Elastic and piezoelectric fields around a buried quantum dot: a simple picture, J. Appl. Phys. 84 (3) (1998) 1358.